



## Spin-dependent tunneling of single electrons into an empty quantum dot

S. Amasha,<sup>1,\*</sup> K. MacLean,<sup>1</sup> Iuliana P. Radu,<sup>1</sup> D. M. Zumbühl,<sup>2</sup> M. A. Kastner,<sup>1</sup> M. P. Hanson,<sup>3</sup> and A. C. Gossard<sup>3</sup>

<sup>1</sup>*Department of Physics, Massachusetts Institute of Technology, Cambridge, Massachusetts 02139, USA*

<sup>2</sup>*Department of Physics, University of Basel, Klingelbergstrasse 82, CH-4056 Basel, Switzerland*

<sup>3</sup>*Materials Department, University of California, Santa Barbara, California 93106-5050, USA*

(Received 13 June 2008; published 28 July 2008)

Using real-time charge sensing and gate pulsing techniques we measure the ratio of the rates for tunneling into the excited and ground spin states of a single-electron quantum dot at an AlGaAs/GaAs interface in a magnetic field parallel to the interface. We find that the ratio decreases with increasing magnetic field until tunneling into the excited spin state is completely suppressed. However, we find that by adjusting the voltages on the surface gates to change the orbital configuration of the dot, we can restore tunneling into the excited spin state and that the ratio reaches a maximum when the dot is symmetric.

DOI: 10.1103/PhysRevB.78.041306

PACS number(s): 73.40.Gk, 73.23.Hk, 73.63.Kv

The spin physics of tunneling in quantum dots<sup>1–7</sup> (QDs) is of great interest because of potential uses for QDs in spin-based applications such as quantum computing<sup>8–11</sup> or spintronic devices<sup>12,13</sup> such as spin filters.<sup>14,15</sup> A lateral QD consists of electrons in a two-dimensional electron gas (2DEG) at the AlGaAs/GaAs interface that are confined in a potential defined by surface gates. In an empty dot, a magnetic field  $B$  applied parallel to the 2DEG splits the spin states of the dot by an energy  $\Delta = |g|\mu_B B$ . For elastic tunneling<sup>16</sup> and no coupling between the electron orbital and spin states in the dot or the leads, we expect the tunneling rates into the two spin states to be equal. This is because in the absence of such coupling, the excited and ground spin states of the dot have the same orbital wave function and hence the same overlap with the leads. Figure 1 illustrates tunneling for spin-up and spin-down electrons. The Hamiltonian for the system is  $H = \frac{p^2}{2m^*} + U_{\text{dot}}(x, y) + \frac{1}{2}\Delta\sigma_y$ , where  $U_{\text{dot}}$  is the electrostatic potential,  $\sigma_y$  is the Pauli-spin matrix, and the magnetic field is applied along the  $y$  axis. The effective potential seen by the electrons is  $U_{\text{eff}} = U_{\text{dot}} + \frac{1}{2}\Delta\sigma_y$  and it is different for the two spin states:  $U_{\text{eff},\downarrow} = U_{\text{eff},\uparrow} + \Delta$ . However, because the bottom of the conduction band is also shifted by  $\Delta$  for spin-down electrons, the spin-up and spin-down electrons tunnel through barriers of equal height and width, and we expect the tunneling rates into the two spin states to be equal.

Here we report the results of using real-time charge sensing and gate pulsing techniques to measure electron tunneling into an empty lateral QD in a magnetic field parallel to the 2DEG. We find that the ratio of the rates for tunneling into the excited and ground spin states depends on the magnetic field and the orbital configuration. Specifically, we find that the ratio decreases with increasing magnetic field until tunneling into the excited spin state is completely suppressed. However, we find that by adjusting the voltages on the surface gates to change the shape of the dot, we can restore tunneling into the excited spin state and that the ratio of the tunneling rates reaches a maximum when the dot is symmetric. These observations imply that the simple picture of electron tunneling described above does not adequately describe the physics of electron tunneling in a magnetic field.

We fabricate our dots from an  $\text{Al}_{0.3}\text{Ga}_{0.7}\text{As}/\text{GaAs}$  heterostructure grown by molecular-beam epitaxy. The 2DEG

formed at the material interface 110 nm below the surface has a density of  $2.2 \times 10^{11} \text{ cm}^{-2}$  and a mobility of  $6.4 \times 10^5 \text{ cm}^2/\text{V s}$ .<sup>17</sup> We pattern Ti/Au gates on the surface as shown in Fig. 2(a). By applying negative voltages to the labeled gates we deplete the 2DEG underneath them and form a single dot containing one electron, as well as a quantum point contact (QPC) between gates SG2 and QG2. The remaining 2DEG regions form the Ohmic leads, two of which are numbered in Fig. 2(a). Electrons tunnel onto and off of the dot through the tunnel barrier defined by gates SG2 and OG while the tunneling rate through the SG1-OG barrier is kept negligibly small. Thus electrons only tunnel between the dot and lead 2, as illustrated in Fig. 2(a). To measure the occupancy of the dot, we use the QPC as a charge sensor.<sup>18</sup> When an electron tunnels onto or off of the dot, it changes the resistance of the QPC and we detect this change by sourcing a current and measuring the change in voltage  $\delta V_{\text{QPC}}$ . By making the tunneling rate slower than the bandwidth of our circuit, we observe electron-tunneling events in real time.<sup>16,19–22</sup> All measurements have been made in a dilution refrigerator with an electron temperature  $T = 120 \text{ mK}$ .

To measure  $\Gamma_{\text{on}}$ , which is the rate at which electrons tunnel onto the dot, we use the two-step pulse sequence shown in Fig. 2(b). The first step is to ionize the dot by pulsing gate LP2 to bring both spin states above the Fermi energy of the lead, so that any electron on the dot tunnels off. During the subsequent load step we apply a positive pulse voltage  $V_p$  (in addition to the negative dc bias voltage) to bring the ground spin state below the Fermi energy of the lead by an energy  $E_p = e\alpha V_p$ , where  $e\alpha$  is a conversion constant we have calibrated separately.<sup>23,24</sup> If only the ground spin state is below the Fermi energy [top diagram in Fig. 2(b)] then  $\Gamma_{\text{on}}$  is equal

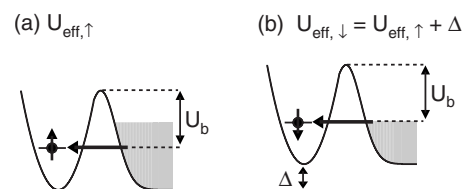


FIG. 1. Tunneling for (a) spin-up and (b) spin-down electrons. Note that both spin species have the same Fermi energy.

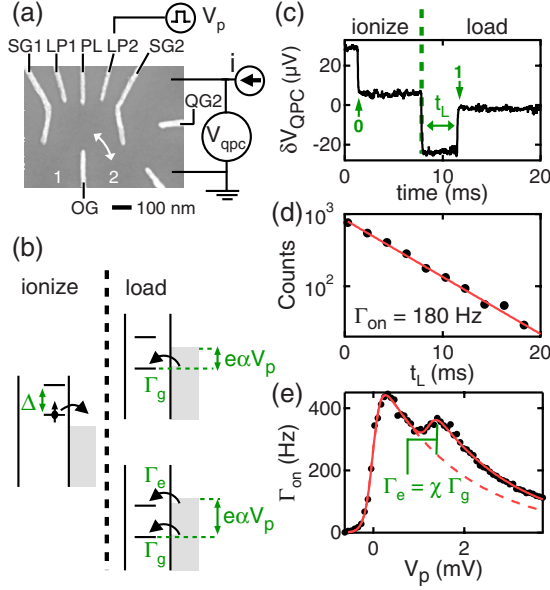


FIG. 2. (Color online) (a) Electron micrograph of the gate geometry. Negative voltages are applied to the labeled gates while the unlabeled gate and the Ohmic leads are kept at ground. Voltage pulses are applied to gate LP2. (b) Dot energy diagrams showing the position of the spin states during the pulse sequence. (c) Example of real-time data. The direct capacitive coupling between LP2 and the QPC causes the QPC to respond to the pulse sequence; electron-tunneling events are evident on top of this response. The 0 denotes when an electron tunnels off the dot, while the 1 denotes when an electron tunnels on. (d) Example of a histogram of  $t_L$  for a given pulse depth. Fitting these data to an exponential (solid line) gives  $\Gamma_{on}$ . (e)  $\Gamma_{on}$  as a function of pulse depth  $V_p$  at  $B=5$  T. The solid and dashed lines are fits discussed in the text to obtain  $\chi = \Gamma_e/\Gamma_g$ .

to the rate for tunneling into the ground state  $\Gamma_g$ . For large enough  $V_p$ , the excited spin state is also below the Fermi energy [bottom diagram in Fig. 2(b)], and then  $\Gamma_{on} = \Gamma_g + \Gamma_e$ , where  $\Gamma_e$  is the rate for tunneling into the excited spin state.

Figure 2(c) shows an example of a pulse sequence taken with our real-time charge detection system. During the ionization step, an electron tunnels off the dot. Then an electron tunnels back onto the dot at a time  $t_L$  after the dot is pulsed into the load state. Figure 2(d) shows a histogram of measurements of  $t_L$  for a fixed  $V_p$ . By fitting these data to an exponential we extract  $\Gamma_{on}$  at this value of  $V_p$ . Figure 2(e) shows an example of  $\Gamma_{on}$  as a function of  $V_p$ . The large increase at  $V_p=0$  corresponds to the ground spin state passing the Fermi level, while the increase at  $V_p \approx 1.5$  mV corresponds to the excited spin state passing the Fermi level.

We use data such as those in Fig. 2(e) to extract the ratio of the rates for tunneling into the spin states. In MacLean *et al.*<sup>16</sup> we showed that the tunneling rate into an empty dot state at  $B=0$  can be described by  $\Gamma = \Gamma_0 e^{-\beta V_p} f(-e\alpha V_p)$ . Here  $\Gamma_0$  is the tunneling rate through the SG2-OG tunnel barrier when the energy of the dot state is aligned with the Fermi energy of the lead, and the exponential factor describes the decrease in the tunneling rate as  $V_p$  pulls the energy of the dot state further below the top of the tunnel barrier. The Fermi function  $f(E) = (1 + e^{E/k_B T})^{-1}$  describes the occupation

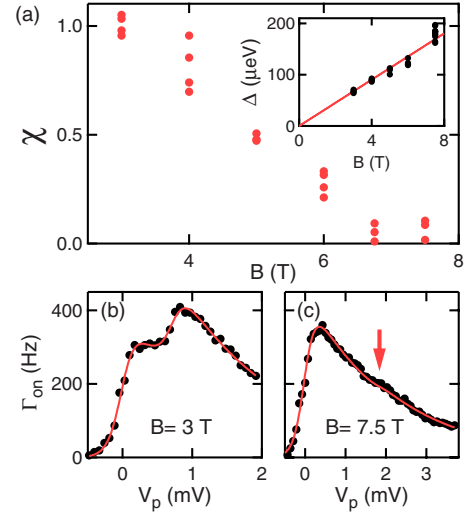


FIG. 3. (Color online) (a)  $\chi$  as a function of magnetic field from fits to data such as those in Fig. 2(e). For  $B \leq 6$  T, the excited-state feature is clearly visible and  $\Delta$  can be extracted from the fit. For  $B > 6$  T, the feature is not visible and fits are performed fixing  $\Delta = |g|\mu_B B$ , where  $|g|=0.39$  is determined by fitting measurements from which we can extract  $\Delta$  (inset). These measurements include values at  $B=7.5$  T for different orbital configurations where tunneling into the excited spin state is not suppressed. (b) Data and the fit (see text) at  $B=3$  T. The increase in the tunneling rate caused by the excited spin state passing below the Fermi energy is clearly visible. (c) Data and the fit at  $B=7.5$  T. The arrow marks the value of  $V_p = \Delta/e\alpha$  where the feature is expected to be.

of states in the lead at the energy of the dot state. In a magnetic field the spin states of the dot are split by  $\Delta$  and we can describe  $\Gamma_{on}$  by

$$\Gamma_{on} = \Gamma_0 e^{-\beta V_p} [f(-e\alpha V_p) + \chi f(-e\alpha V_p + \Delta)], \quad (1)$$

where  $f(-e\alpha V_p)$  and  $f(-e\alpha V_p + \Delta)$  describe the occupation of the lead at the energies of the ground and excited spin states, respectively. The solid line in Fig. 2(e) shows a fit to Eq. (1), and there is good agreement with the data. The dashed line shows the contribution of tunneling into the ground spin state, given by  $\Gamma_g = \Gamma_0 e^{-\beta V_p} f(-e\alpha V_p)$ , while the remaining contribution is caused by tunneling into the excited spin state  $\Gamma_e$ . When both spin states are below the Fermi energy such that  $f(-e\alpha V_p) \approx f(-e\alpha V_p + \Delta) \approx 1$  then  $\chi$  is the ratio of the rates  $\chi = \Gamma_e/\Gamma_g$ . In the simple picture of tunneling presented above, both spin states of the dot have the same orbital wave function, so the tunneling rates should have the same dependence on  $V_p$  and we expect that  $\chi=1$ .

Figure 3(a) shows measurements of  $\chi$  obtained by fitting line shapes at different magnetic fields. Figures 3(b) and 3(c) show examples of data at  $B=3$  and 7.5 T, respectively. In Fig. 3(b) the increase in  $\Gamma_{on}$  caused by the excited spin state passing the Fermi energy is clearly visible. In Fig. 3(c) no increase is visible; the arrow marks the value of  $V_p = \Delta/e\alpha$  where the feature should be. From Fig. 3(a), we see that application of a magnetic field suppresses the tunneling rate  $\Gamma_e$  into the excited spin state, relative to that into the ground state.<sup>25</sup>

We can change this suppression by varying the voltages on the gates that define the dot.<sup>23</sup> Figure 4(a) defines the  $x$  and  $y$  axes, which are aligned with the  $[110]$  and  $[\bar{1}10]$  GaAs crystalline axes, respectively. When the voltages on all dot gates are approximately equal, we expect from the gate geometry that the dot is less confined along  $x$  than along  $y$  [black solid ellipse in Fig. 4(a)]. We change the shape of the dot by applying a more negative voltage to SG1, which pushes the dot wave function toward SG2, thereby increasing confinement along  $x$ . Simultaneously, we make the voltages on LP1, PL, and LP2 less negative which reduces confinement along  $y$  [white dotted ellipse in Fig. 4(a)], while keeping the ground orbital state energy constant. We parameterize a set of gate voltages by  $V_{\text{shape}}$ , the numeric value of which is the voltage on gate SG1.

To characterize the change in shape of the dot we use the energies of the excited orbital states.<sup>23</sup> We can model the electrostatic potential of the dot with an anisotropic harmonic-oscillator potential  $U(x, y) = \frac{1}{2}m^*\omega_x^2x^2 + \frac{1}{2}m^*\omega_y^2y^2$ . Then the energies  $E_x$  and  $E_y$  of the  $x$ -like and  $y$ -like excited orbital states relative to the ground orbital state are determined by the confinement:  $E_x = \hbar\omega_x$  and  $E_y = \hbar\omega_y$ . For less negative  $V_{\text{shape}}$  the dot is less confined along  $x$  than along  $y$  so we expect  $E_x < E_y$ . As we make  $V_{\text{shape}}$  more negative we increase the confinement along  $x$  and decrease the confinement along  $y$ , and so we expect that  $E_x$  should increase and  $E_y$  should decrease as  $V_{\text{shape}}$  is made more negative.

The top panel of Fig. 4(b) shows the energies of the first two excited orbital states of the dot measured using gate pulsing and real-time charge detection techniques at  $B = 0$  T.<sup>23</sup> As expected, the energy of one orbital state increases and that of the other orbital state decreases as  $V_{\text{shape}}$  is made more negative, and this allows us to identify the states as indicated in the top panel of Fig. 4(b). At each value of  $V_{\text{shape}}$  we perform measurements of  $\chi$  at  $B = 7.5$  T as in Fig. 3(c), and the results are shown in the bottom panel of Fig. 4(b). The data in Fig. 3 have been taken at the most negative value of  $V_{\text{shape}} = -1350$  mV. Making  $V_{\text{shape}}$  less negative [Fig. 4(b)] changes  $\chi$ , and  $\chi$  reaches a maximum of  $\approx 1$  at  $V_{\text{shape}} \approx -990$  mV when the dot is symmetric. Figure 4(c) shows data taken at the  $V_{\text{shape}}$  for a symmetric dot. In contrast to Fig. 3(c) the excited spin state is now clearly visible. At each value of  $V_{\text{shape}}$ , we check that electrons only tunnel between the dot and lead 2. From measurements of  $\Gamma_{\text{on}}$  vs  $V_p$  for which the excited spin state feature is visible ( $V_{\text{shape}} > -1300$  mV), we can extract  $\Delta$  at  $B = 7.5$  T and we find that  $\Delta$  is independent of  $V_{\text{shape}}$  within experimental error.

That  $\chi$  changes with the magnetic field and with the shape of the dot imply that the simple picture given above, of electron tunneling in a magnetic field, is not adequate. One explanation we have considered is the presence of a magnetic field  $B_{\perp}$  perpendicular to the 2DEG that is caused by misalignment of the sample. We estimate that this sample is parallel to within  $5^\circ$  and this limits  $B_{\perp} < 0.65$  T at  $B = 7.5$  T. Since we are measuring single-electron tunneling into an empty dot, there are no exchange effects in the dot; rather, the dot states are single-particle states. However,  $B_{\perp}$  can affect the states in the Ohmic leads by forming Landau levels, and one possibility is that we would observe spin-

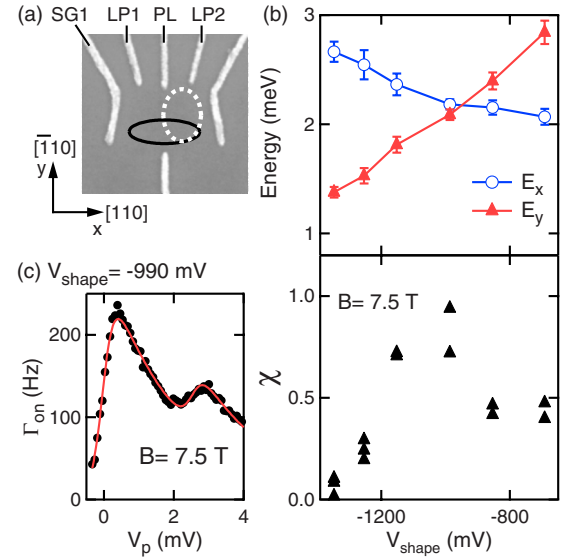


FIG. 4. (Color online) (a) The black solid (white dotted) ellipse illustrates the expected dot shape for less (more) negative  $V_{\text{shape}}$ . For all data in this paper, the magnetic field is applied along the  $y$  axis. (b) The top panel shows the energy spectrum of the excited orbital states as a function of  $V_{\text{shape}}$ . The bottom panel shows  $\chi$  measured at  $B = 7.5$  T for each value of  $V_{\text{shape}}$ . (c) Data at  $V_{\text{shape}} = -987$  mV and  $B = 7.5$  T. Unlike Fig. 3(c), at this value of  $V_{\text{shape}}$  the excited spin state feature is clearly present. The value of  $V_p$  at which it appears is different than in Fig. 3(c) because the conversion constant  $e\alpha$  changes with  $V_{\text{shape}}$ .

dependent tunneling because the dot acts as a spin-sensitive probe of the states in the leads.<sup>1</sup> We do not believe this is the case because this mechanism does not explain how changes in the dot shape could affect  $\chi$ . Also, we have observed spin-dependent tunneling in a second device, where we estimate  $B_{\perp} \sim 20$  mT at  $B = 7.5$  T based on a Hall voltage measurement: this precludes Landau level quantization.

We have also considered the effects of the spin-orbit interaction (SOI) in both the dot and the leads. The effect of the SOI on the dot states is small because it is on the order of  $x/\lambda_{\text{SO}} \approx 8 \times 10^{-3}$ , where  $x \approx 17$  nm is the length scale for a harmonic-oscillator potential approximating a dot with orbital energy spacing  $E \approx 2$  meV, and the spin-orbit length  $\lambda_{\text{SO}} \sim 2$   $\mu\text{m}$  describes the strength of the SOI.<sup>23,26</sup> In the leads the SOI can be thought of as a momentum-dependent effective magnetic field  $B_{\text{SO}}$  which is  $\approx 6$  T at the Fermi energy using  $\lambda_{\text{SO}} \sim 2$   $\mu\text{m}$ . As the magnetic field increases we expect the Zeeman splitting to begin to dominate the SOI and the physics to approach the simple picture discussed above, so that  $\chi$  should approach 1 at high fields. This is not what we observe.

Measurements of other aspects of tunneling in lateral dots in parallel magnetic fields have also given results that differ from what is expected based on simple considerations, such as those in Fig. 1. Potok *et al.*<sup>3</sup> have measured the spin polarization of electrons tunneling out of a lateral dot in a parallel magnetic field. Naively, one would expect the spin polarization to depend on the spin state of the dot. However, these authors have observed no variation in the spin polarization of the emitted electron as they varied the spin state of

the dot. Taken in conjunction with our results, it appears that the experimental picture of the spin dependence of tunneling in lateral QDs is very different from what one expects based on simple considerations.

In summary, we find that the ratio of the rates for a single electron tunneling into the excited and ground spin states of an empty quantum dot decreases with increasing magnetic field and that the ratio reaches a maximum when the dot is symmetric. We know no theoretical explanation for these observations, which underscores the fact that understanding the spin-dependence of tunneling continues to be an important

open problem in the physics of quantum dots.

We are grateful to D. Loss, L. Levitov, E. I. Rashba, J. B. Miller, and O. Dial for discussions and to I. J. Gelfand and T. Mentzel for experimental help. This work was supported by the U.S. Army Research Office under Contract No. W911NF-05-1-0062, by the National Science Foundation under Contract No. DMR-0353209, and in part by the NSEC Program of the National Science Foundation under Contract No. PHY-0117795. D.M.Z. acknowledges financial support from the Swiss Nanoscience Institute.

\*Current address: Department of Physics, Stanford University, Stanford, California 94305, USA: samasha@stanford.edu

- <sup>1</sup>M. Ciorga, A. S. Sachrajda, P. Hawrylak, C. Gould, P. Zawadzki, S. Jullian, Y. Feng, and Z. Wasilewski, *Phys. Rev. B* **61**, R16315 (2000).
- <sup>2</sup>S. Lindemann, T. Ihn, T. Heinzel, W. Zwerger, K. Ensslin, K. Maranowski, and A. C. Gossard, *Phys. Rev. B* **66**, 195314 (2002).
- <sup>3</sup>R. M. Potok, J. A. Folk, C. M. Marcus, V. Umansky, M. Hanson, and A. C. Gossard, *Phys. Rev. Lett.* **91**, 016802 (2003).
- <sup>4</sup>K. Hitachi, M. Yamamoto, and S. Tarucha, *Phys. Rev. B* **74**, 161301(R) (2006).
- <sup>5</sup>O. Zarchin, Y. C. Chung, M. Heiblum, D. Rohrlich, and V. Umansky, *Phys. Rev. Lett.* **98**, 066801 (2007).
- <sup>6</sup>I. Hapke-Wurst, U. Zeitler, H. Frahm, A. G. M. Jansen, R. J. Haug, and K. Pierz, *Phys. Rev. B* **62**, 12621 (2000).
- <sup>7</sup>E. E. Vdovin, Y. N. Khanin, O. Makarovskiy, Y. V. Dubrovskii, A. Patanè, L. Eaves, M. Henini, C. J. Mellor, K. A. Benedict, and R. Airey, *Phys. Rev. B* **75**, 115315 (2007).
- <sup>8</sup>D. Loss and D. P. DiVincenzo, *Phys. Rev. A* **57**, 120 (1998).
- <sup>9</sup>R. Hanson, L. P. Kouwenhoven, J. R. Petta, S. Tarucha, and L. M. K. Vandersypen, *Rev. Mod. Phys.* **79**, 1217 (2007).
- <sup>10</sup>J. R. Petta, A. C. Johnson, J. M. Taylor, E. A. Laird, A. Yacoby, M. D. Lukin, C. M. Marcus, M. P. Hanson, and A. C. Gossard, *Science* **309**, 2180 (2005).
- <sup>11</sup>F. H. L. Koppens, C. Buizert, K. J. Tielrooij, I. T. Vink, K. C. Nowack, T. Meunier, L. P. Kouwenhoven, and L. M. K. Vandersypen, *Nature (London)* **442**, 766 (2006).
- <sup>12</sup>I. Žutić, J. Fabian, and S. Das Sarma, *Rev. Mod. Phys.* **76**, 323 (2004).
- <sup>13</sup>D. D. Awschalom and M. E. Flatté, *Nat. Phys.* **3**, 153 (2007).
- <sup>14</sup>J. A. Folk, R. M. Potok, C. M. Marcus, and V. Umansky, *Science* **299**, 679 (2003).
- <sup>15</sup>R. Hanson, L. M. K. Vandersypen, L. H. Willems van Beveren, J. M. Elzerman, I. T. Vink, and L. P. Kouwenhoven, *Phys. Rev. B* **70**, 241304(R) (2004).
- <sup>16</sup>K. MacLean, S. Amasha, I. P. Radu, D. M. Zumbühl, M. A. Kastner, M. P. Hanson, and A. C. Gossard, *Phys. Rev. Lett.* **98**, 036802 (2007).
- <sup>17</sup>G. Granger, M. A. Kastner, I. Radu, M. P. Hanson, and A. C. Gossard, *Phys. Rev. B* **72**, 165309 (2005).
- <sup>18</sup>M. Field, C. G. Smith, M. Pepper, D. A. Ritchie, J. E. F. Frost, G. A. C. Jones, and D. G. Hasko, *Phys. Rev. Lett.* **70**, 1311 (1993).
- <sup>19</sup>W. Lu, Z. Ji, L. Pfeiffer, K. W. West, and A. J. Rimberg, *Nature (London)* **423**, 422 (2003).
- <sup>20</sup>J. M. Elzerman, R. Hanson, L. H. Willems van Beveren, B. Witkamp, L. M. K. Vandersypen, and L. P. Kouwenhoven, *Nature (London)* **430**, 431 (2004).
- <sup>21</sup>R. Hanson, L. H. Willems van Beveren, I. T. Vink, J. M. Elzerman, W. J. M. Naber, F. H. L. Koppens, L. P. Kouwenhoven, and L. M. K. Vandersypen, *Phys. Rev. Lett.* **94**, 196802 (2005).
- <sup>22</sup>S. Gustavsson, R. Leturcq, B. Simović, R. Schleser, T. Ihn, P. Studerus, K. Ensslin, D. C. Driscoll, and A. C. Gossard, *Phys. Rev. Lett.* **96**, 076605 (2006).
- <sup>23</sup>S. Amasha, K. MacLean, I. P. Radu, D. M. Zumbühl, M. A. Kastner, M. P. Hanson, and A. C. Gossard, *Phys. Rev. Lett.* **100**, 046803 (2008).
- <sup>24</sup>S. Gustavsson, R. Leturcq, B. Simović, R. Schleser, P. Studerus, T. Ihn, K. Ensslin, D. C. Driscoll, and A. C. Gossard, *Phys. Rev. B* **74**, 195305 (2006).
- <sup>25</sup>The bare tunneling rate onto the dot  $\Gamma_0$  changes with magnetic field and hence it is necessary to adjust this rate using the gate voltages to keep  $\Gamma_{\text{on}}$  at measurable levels ( $\approx 200\text{--}400$  Hz at the peak). This means it is not possible to compare the values of  $\Gamma_{\text{on}}$  at two different magnetic fields. Consequently we cannot determine whether the decrease in  $\chi$  is caused by an increase in  $\Gamma_g$  or a decrease in  $\Gamma_e$ .
- <sup>26</sup>D. M. Zumbühl, J. B. Miller, C. M. Marcus, K. Campman, and A. C. Gossard, *Phys. Rev. Lett.* **89**, 276803 (2002).